J Braz. Soc. Mech. Sci. Eng. (2017) 39:601–611
DOI 10.1007/s40430-016-0522-x

TECHNICAL PAPER

Stress intensity factors of corner cracks at set-in nozzle–cylinder intersection of a PWR reactor pressure vessel

Usman Tariq Murtaza[1] · **M. Javed Hyder**[1]

Received: 22 October 2014 / Accepted: 3 March 2016 / Published online: 18 March 2016

Abstract Reactor pressure vessel (RPV) is the central and the most important component of a pressurized water reactor (PWR). The fracture mechanics analysis of different parts of the RPV under various loading conditions is compulsory as it is not always possible to manufacture a crack- or defect-free component. The strength of a crack, in an engineering component, is normally evaluated by computing the stress intensity factors (SIFs) along the crack front. In this paper, for the fracture mechanics analysis of the set-in nozzle of a 300-MW RPV, the SIFs of a wide range of corner surface cracks at the nozzle–cylinder intersection are being presented. The considered RPV is made of a nuclear-grade steel designated as 'SA-508 Gr.3 Cl.1'. The analyzed corner cracks are in the range of '$0.01 < a/t < 0.25$' and '$0.33 < a/c < 1.0$', where 'a' and 'c' represent minor and major axes of the crack, respectively; and 't' is the thickness of the vessel wall at the nozzle–cylinder intersection. In this study, both the linear elastic fracture mechanics (LEFM) and elasto-plastic fracture mechanics (EPFM) based SIFs are provided under normal operating conditions of the plant. The shape and size of the plastic zone at the crack tip, using von Mises failure criterion, is also presented.

Keywords Corner crack · SIF · RPV · ANSYS

Nomenclature

PWR	Pressurized water reactor
RPV	Reactor pressure vessel
ASME	American Society of Mechanical Engineering
LEFM	Linear elastic fracture mechanics
EPFM	Elasto-plastic fracture mechanics
SIF	Stress intensity factor
HSCP	Highest stress concentration point
a	Minor axis of the corner crack
c	Major axis of the corner crack
t	Thickness of the vessel's wall at nozzle–cylinder intersection
E	Young modulus of the material
P_{int}	Internal pressure
ϕ	Crack face angle, degrees
α	Angle between set-in and set-out nozzles
ρ	Density of the material
ν	Poisson's ratio of the material
σ_{ys}	Yield strength of the material
R_m	Mean radius of the nozzle's belt
K^P_{IN}	LEFM-based SIF under normal operating conditions
K^P_{JN}	EPFM-based SIF under normal operating conditions

1 Introduction

Pressurized water reactor (PWR) is one of the popular reactor types which are being used for power production. Reactor pressure vessel (RPV) [1, 2] is one of the important components used in the primary loop of the PWR. The RPV is a 'class 1' of the power plant according to the definition of ASME code [3]. The fracture mechanics analysis of different parts of the RPV, e.g., set-in nozzle, set-out

Technical Editor: Lavinia Maria Sanabio Alves Borges.

✉ Usman Tariq Murtaza
maniiut@yahoo.com

[1] Department of Mechanical Engineering, Pakistan Institute of Engineering and Applied Sciences, Islamabad 45650, Pakistan

nozzle and nozzle-belt region, is highly recommended [4] before starting the operation of the plant. The analysis is compulsory because the components may have minute manufacturing defects or cracks, or some inherent material flaws. The behavior of a component having such defects confirms whether the defects can be tolerated or not; and if they can be tolerated then what is the safety factor of the component. In this study, for the fracture mechanics analysis of a set-in nozzle of an RPV, a wide range of the corner surface cracks have been analyzed at the nozzle–cylinder intersection of the vessel. The behavior of the cracks, in the form of stress intensity factor (SIFs), have been computed under normal operating conditions of the plant.

1.1 Goal of the research work

The effects of material plasticity on the SIFs of the corner cracks have mainly been investigated in this study. For this purpose, both linear elastic fracture mechanics (LEFM) based SIFs; and elasto-plastic fracture mechanics (EPFM) based SIFs are being presented in this paper. Secondly, the LEFM-based SIFs have also been normalized for investigating the strength of the cracks at the nozzle–cylinder intersection in comparison to normal cylindrical sections.

1.2 Need of the research work

The problem encountered, in this study, is of industrial nature which needs to be investigated. The explored effects and the results were missing in the contemporary literature and therefore a research work was required in order to close this lacuna.

1.3 Crack modeling approach

A pallet body approach for the assessment of corner cracks using ANSYS Workbench was developed in our previous works [5–7]. The approach [5] is as valid as Newman and Raju analysis [8] and ASME code [9] for the computations of stress intensity factors. In this study, in order to compute SIFs of the corner cracks at the nozzle–cylinder intersection, the fracture model of the RPV was developed using the pallet body approach. The approach generates refine brick mesh in the annular region around the crack front. The remaining structure of the component except the annular region around the crack front can be meshed using a free tetrahedral grid of quite larger size. With the use of the pallet body approach, it has been possible to analyze a full three-dimensional RPV having a minute crack at its nozzle.

2 Problem description

2.1 Geometry of the RPV

Figure 1 depicts a typical double-loop cylindrical reactor pressure vessel [10] of a 300 megawatts (MW) pressurized water reactor. Figure 1a shows the cut-section view through the set-in and the set-out nozzles of the RPV; while Fig. 1b shows the top view of the vessel. The pressurized reactor's coolant enters the RPV through the set-in nozzle, and leaves the RPV through the set-out nozzle. The presented RPV has two set-in and two set-out nozzles. The angle between the inlet and outlet nozzles is 60° and it is denoted by 'α' as shown in Fig. 1b. The typical design of the set-in nozzle used in such RPV is shown in Fig. 2. In this study, the stress intensity factors of the corner cracks postulated at the nozzle–cylinder intersection (see Fig. 2) will be presented. The nozzle has a 6° taper angle at the nozzle–cylinder intersection. The thickness of the vessel's wall at the nozzle–cylinder intersection is '$t = 400$ mm'.

2.2 Boundary conditions

The following boundary conditions (BCs) in view of the normal operating conditions of the plant have been applied for this analysis.

1. Taking the advantage of the geometric and loading symmetry, as shown in Fig. 1b, only half of the RPV was modeled for the analysis. The half of the vessel contains one set-in nozzle and one set-out nozzle.
2. The mass of the full RPV, with the material 'SA-508 Gr.3 Cl.1' is 239.70 tonne. The effects of the weight of the vessel have also been considered in the analysis.
3. The RPV is supported by 'support pads' which are provided under the nozzles (see Fig. 1b). The support pads are free to move in tangential and radial directions of the RPV (see Fig. 1b) while they are fixed along the vertical direction of the vessel. In ANSYS Workbench, frictionless support feature was applied on the lower faces of the vessel's support pads. It prevents the supports from moving in the vertical direction of the vessel and allows their movement in the radial and tangential directions of the vessel.
4. Along with the support pads, in order to properly support the heavy RPV, the skirt type support is also recommended at the lower hemisphere of the vessel [11]. The lower hemisphere of the RPV was fixed in the analysis in order to incorporate the effects of skirt support. This assumption is valid in our case because the skirt support has negligible effects on the nozzles.

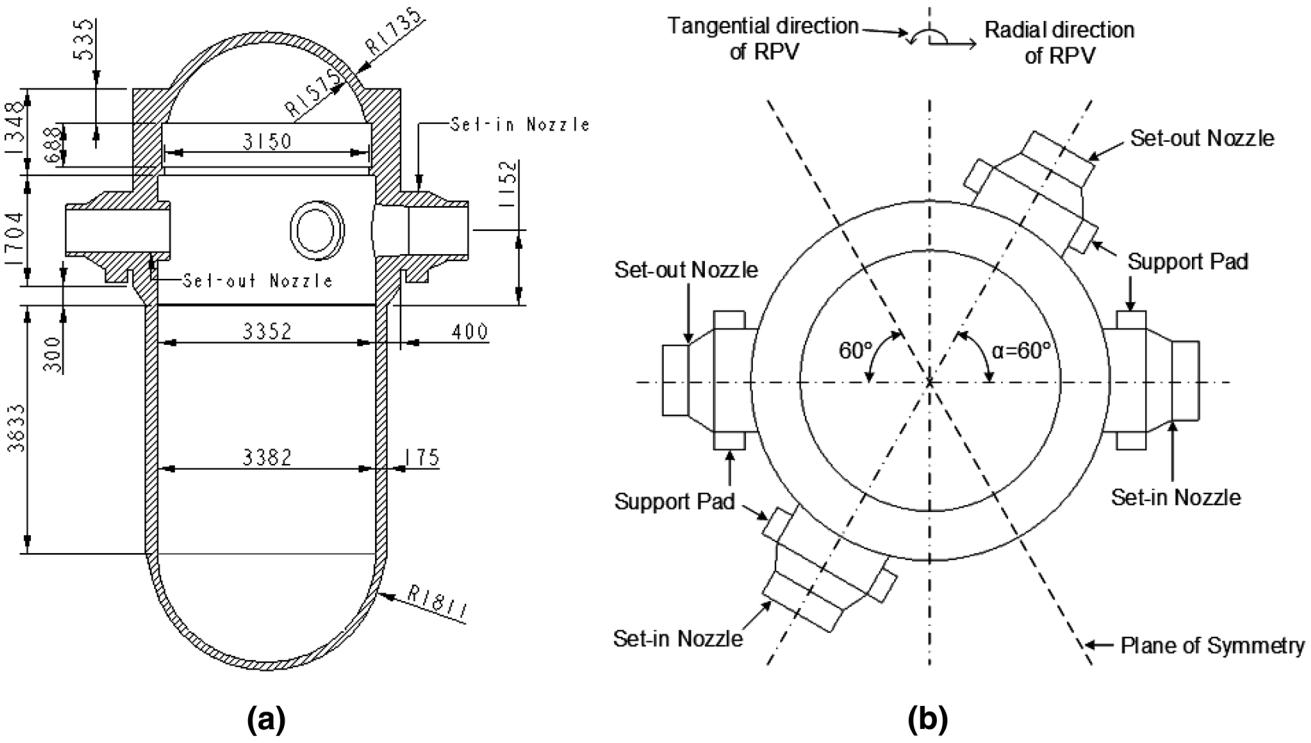

Fig. 1 Engineering drawing of the typical RPV [10], dimensions in mm. **a** Cut-section view and **b** top view

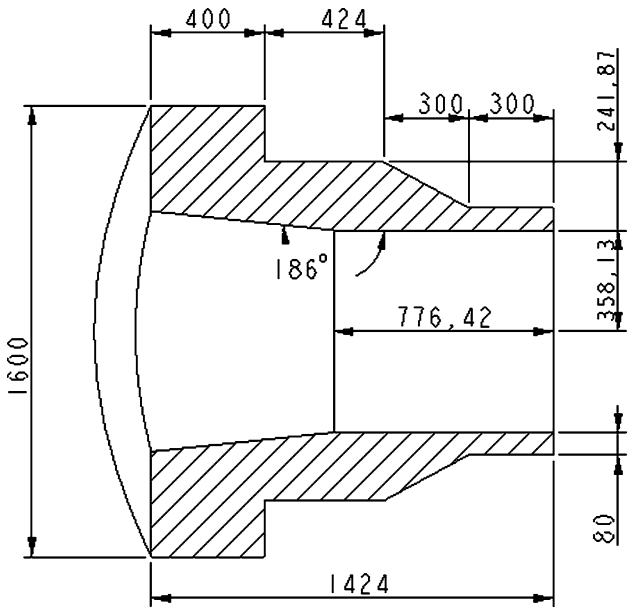

Fig. 2 Typical design of the set-in nozzle [10]

5. The internal pressure equals to 17.16 MPa ($P_{\text{int}} = 17.16$ MPa) is applied to the RPV. This is the design pressure [12] of the RPV.
6. The behavior of the material at $T = 350$ °C is used. This is the design temperature [12] of the RPV.

Table 1 Mechanical properties of the material [14]

Mechanical property	Value
Density, ρ	7750 kg/m^3
Young's modulus, E	171 GPa
Poisson's ratio, ν	0.30
Yield strength	285 MPa

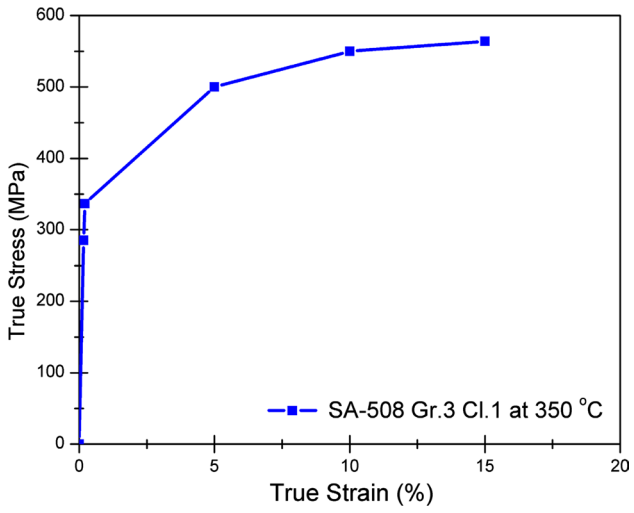

Fig. 3 True stress–strain characteristics [12]

7. The bending loads caused by the support pads on the nozzles have been taken into account.
8. The effects of axial loads on the nozzles have also been considered. These effects are negligible [13], because the support pads are free to move in the axial direction of the nozzle.

2.3 Material model of the RPV

A nuclear-grade steel, designated 'SA-508 Gr.3 Cl.1' (as per ASME code), has been used as the material of the RPV [14]. The nominal composition of the steel is 3/4Ni-1/2Mo-Cr-V. The elastic properties of the steel at the design temperature of the RPV are given in Table 1.

The elastic plastic characteristics of the nuclear-grade steel at the design temperature of the vessel is shown in Fig. 3.

3 The stress analysis of the RPV

In order to compute hoop stress distributions in the uncracked RPV, the symmetrically half of the vessel was meshed using hexahedral finite elements (FE). The meshing was performed using slicing and dicing technique [5] in 'ANSYS DesignModeler'. The full 3D finite element (FE) hex mesh model of the RPV having skewness equal to 0.854 is shown in Fig. 4. The element type used for the development of the FE model is Solid-186. The FE model contains a total of 41,988 finite elements and 203,848 nodes.

The hoop stress distributions under the normal loading conditions of the plant (see "Sect. 2.2") are shown in Fig. 5. It is evident from the contours that the set-in nozzle–cylinder intersection of the RPV is also the highest stress concentration point (HSCP) of the vessel. The corner cracks normal to hoop stresses will be postulated at this HSCP for the computations of SIFs.

4 Numerical calculation of the SIFs

For the computations of SIFs of the cracks in the limits of '$0.01 < a/t < 0.25$' and '$0.33 < a/c < 1.0$', 48 corner cracks of different dimensions were postulated at the nozzle–cylinder intersection. As already mentioned 'a', 'c', and 't' represent minor axis of the crack, major axis of the crack, and thickness of the vessel's wall at nozzle–cylinder intersection, respectively. The orientation of the corner cracks is shown in Fig. 6a; while the crack tip position parameters (a, c, and ϕ) are shown in Fig. 6b.

For the presentation of the SIFs in a suitable graphical format, the corner cracks have been divided into six

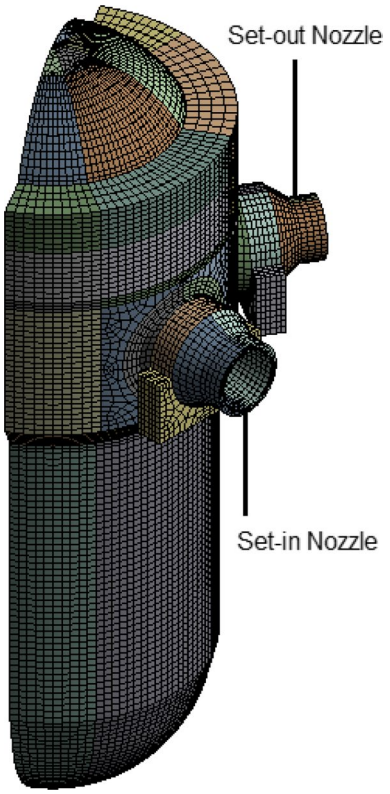

Fig. 4 3D solid-186 finite elements model of the RPV

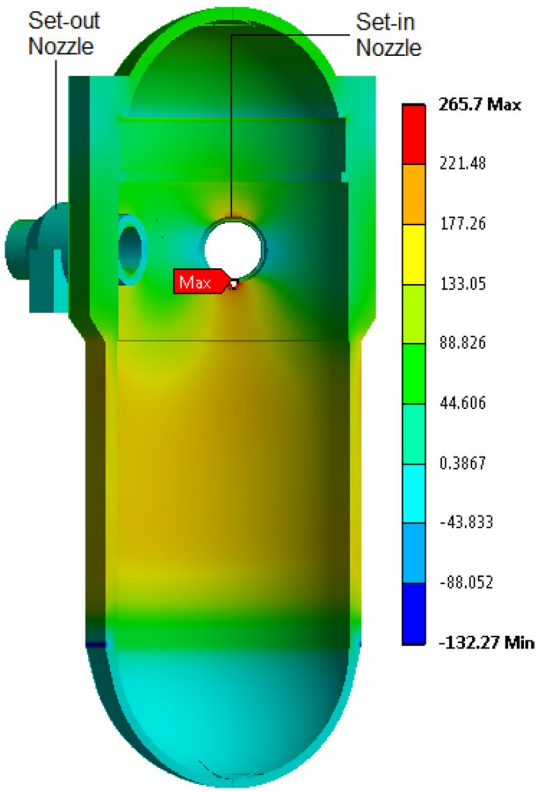

Fig. 5 The hoop stresses (MPa) in the RPV

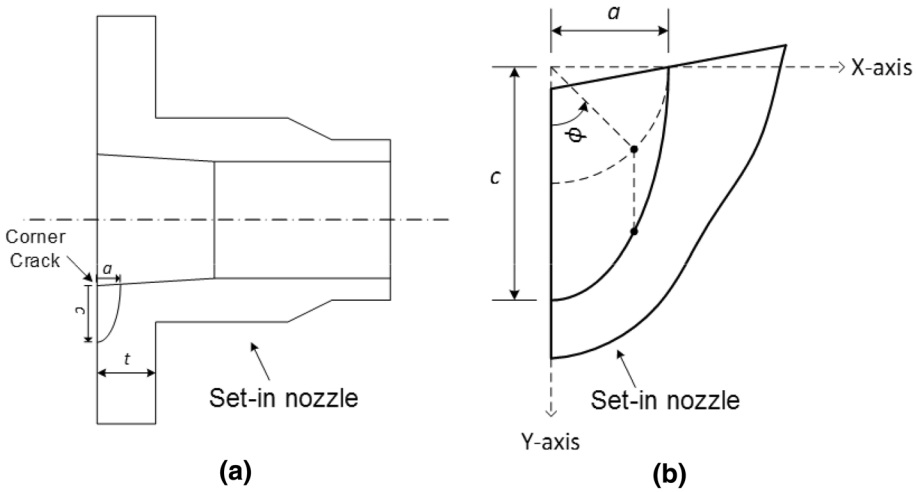

Fig. 6 **a** Orientation of the corner crack and **b** crack tip position parameters

Table 2 The sets of the corner cracks

Set	*a/t* ratio	Elliptical crack, *a/c* ratio	Circular crack, *a/c* ratio
1	0.01	0.33, 0.40, 0.50, 0.60, 0.70, 0.80, 0.90	1.0
2	0.05		
3	0.10		
4	0.15		
5	0.20		
6	0.25		

sets. Each set has a different '*a/t*' ratio. In each set of the cracks, there are eight different cracks of different aspect ratio (*a/c*). Each set has seven elliptical corner cracks ($a/c \neq 1.0$); and one circular corner crack ($a/c = 1.0$). The details of the sets of the cracks are given in Table 2.

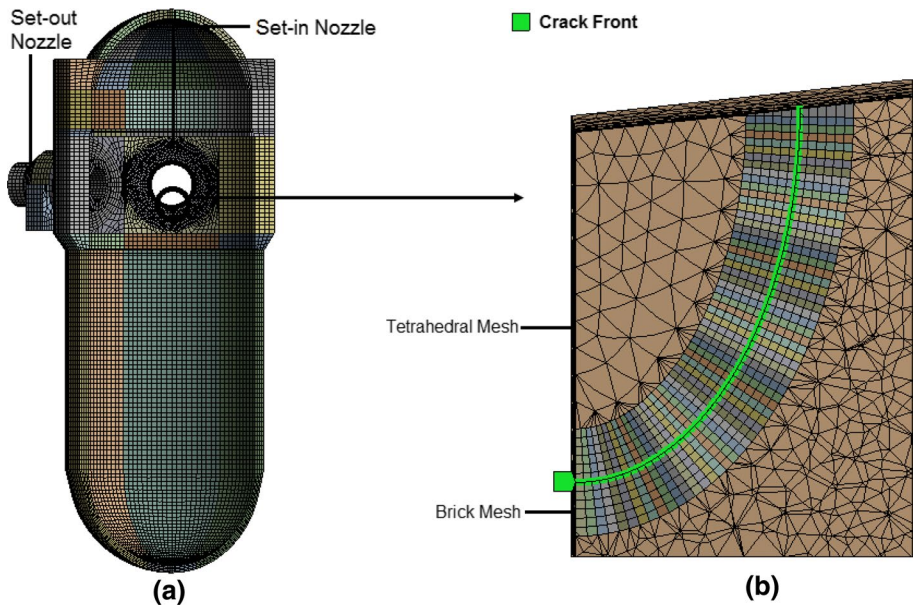

Fig. 7 **a** The pallet body fracture model of the RPV and **b** close-up view of the cracked region

Table 3 Details of finite element fracture model of the RPV

Region	Element type	No. of elements	No. of nodes	No. of layers	No. of pallets
The tube around the crack front	Solid-186	4320	18,709	06	60
Half of the RPV including the tube	Solid-187 and Solid-186	109,225	175,583	06	60

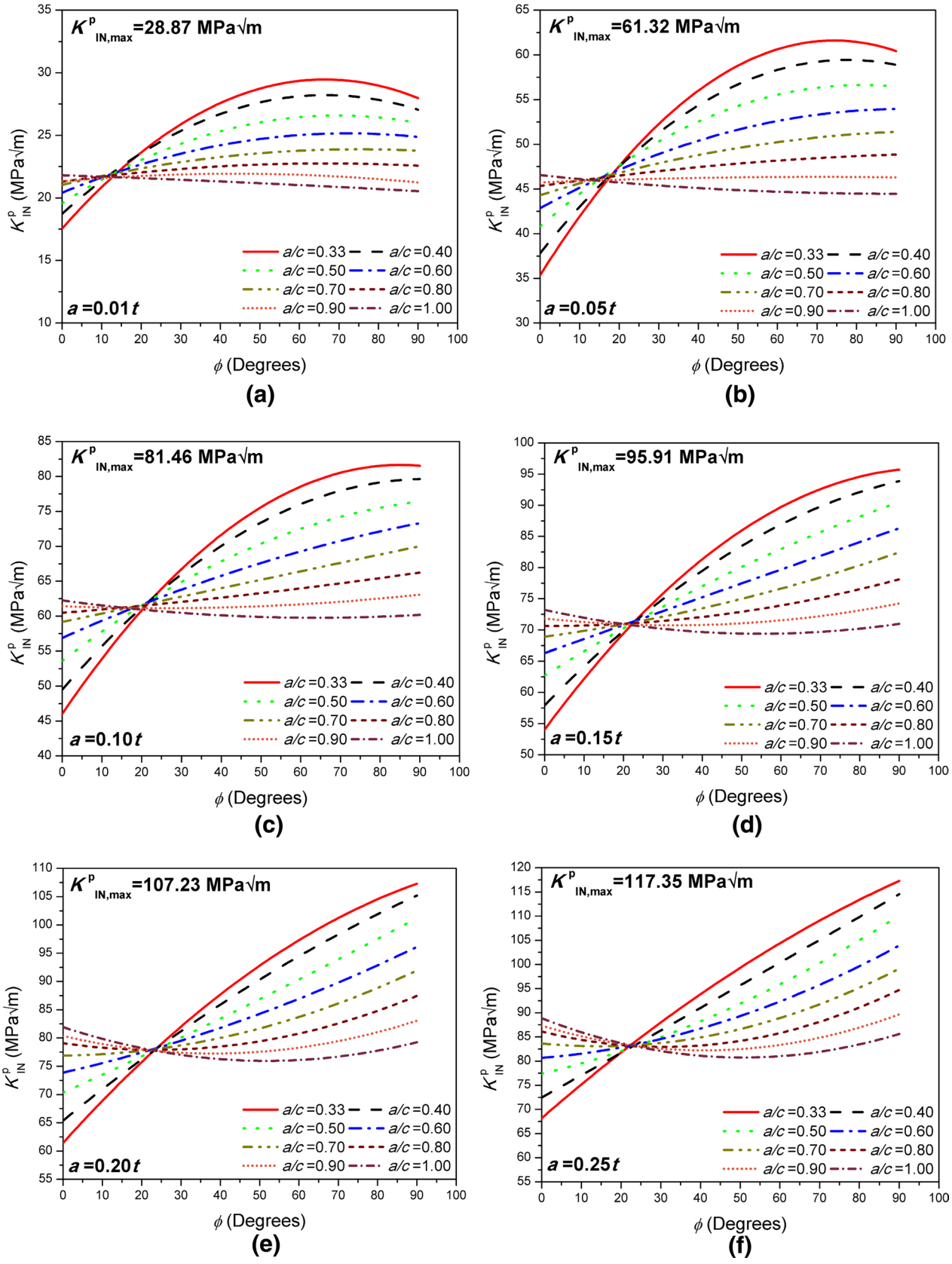

Fig. 8 The 'LEFM-based SIFs' along the fronts of the corner cracks

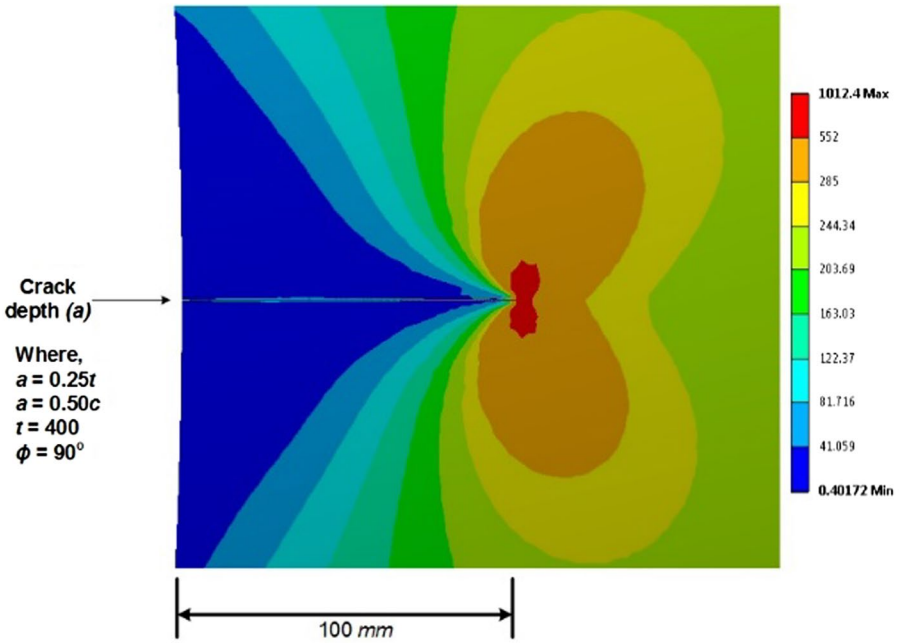

Fig. 9 Plastic zone using Von Mises failure criteria

4.1 Fracture model of the RPV

The 'pallet body fracture model' [5] of the RPV having corner crack ($a = 0.25t$ and $a = 0.33c$) at the nozzle–cylinder intersection is shown in Fig. 7. The close-up view of the cracked region is shown in Fig. 7a. The details of the finite element fracture model in terms of element type, no. of elements, and no. of nodes are given in Table 3.

4.2 The LEFM-based SIFs

The LEFM-based SIFs under normal operating conditions K^P_{IN}, for all the 48 cracks listed in Table 2 are presented in Fig. 8a–f. The linear elastic material model (see Table 1) was used for the computations of these SIFs. Figure 8a–f presents the LEFM-based SIFs of the cracks having minor axis (a) equal to 1, 5, 10, 15, 20 and 25 % of the wall thickness (t), respectively.

It is evident from Fig. 8a–f that all the elliptical corner cracks have varying SIFs along the whole crack fronts from $\phi = 0°$ to 90°. However, the circular corner cracks have almost constant SIFs along the crack fronts. It is also clear that as the 'a/c' ratio increases (for all values of 'a/t'), SIFs at $\phi = 0°$ also increases while SIFs at $\phi = 90°$ decreases. The maximum SIF of the worst crack ($a = 0.25t$ and $a = 0.33c$) approaches the value $K^P_{\mathrm{IN,max}} = 117.35\ \mathrm{Mpa}\sqrt{\mathrm{m}}$ as shown in Fig. 8f.

It is evident from the trends in Fig. 8a–f that at specific angle (which is different for each crack) the slope of SIFs curve changes. This fact validates that that the elliptical crack is the intersection of two curvatures: the minor axis and the major axis of the ellipse.

4.3 The size and shape of the plastic zone

The size and shape of the plastic zone at the tip ($\phi = 90°$) of the crack ($a = 0.25t$ and $a = 0.50c$) is also presented in Fig. 9. The plastic zone has been computed using the Von Mises yielding criterion [15, 16]. The yield strength of the RPV's material at the design temperature is 285 MPa (see Table 1); and hence the Von Mises stresses more than 285 MPa will generate yielding of the material.

Clearly, the size of the plastic zone is smaller than the depth of the crack ($a = 0.25t = 100$ mm). However, the size of the plastic zone is comparable to the thickness of the vessel's wall which is $t = 400$ mm. The comparable size of the plastic zone to the ligament [17] indicates that the small-scale yielding condition [18] is not satisfied in the case of RPV made of 'SA-508 Gr.3 Cl.1' steel. This observation leads to the fact that the 'LEFM-based SIFs' are not sufficient solutions for the fracture evaluation of the RPV. Hence, the 'EPFM-based SIFs' are essentially required which are also being presented in the following section.

4.4 The EPFM-based SIFs

The 'EPFM-based SIFs' (K^P_{JN}) for all the 48 cracks listed in Table 2 are presented in Fig. 10. The elastic plastic material characteristics (see Fig. 3) of the RPV's steel were used for the computations of the 'EPFM-based SIFs'. Figure 10a–f

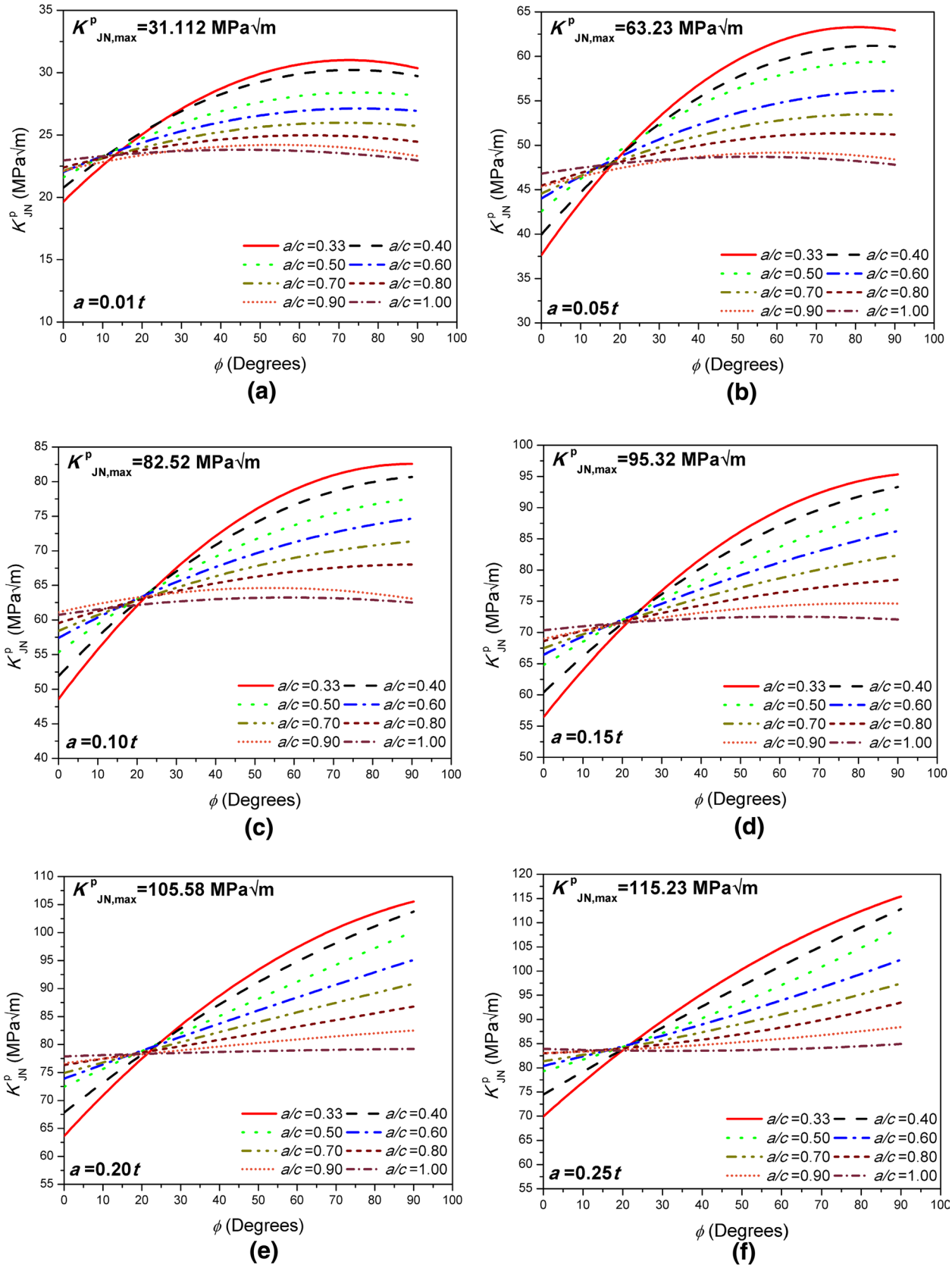

Fig. 10 The 'EPFM-based SIFs' along the fronts of the corner cracks

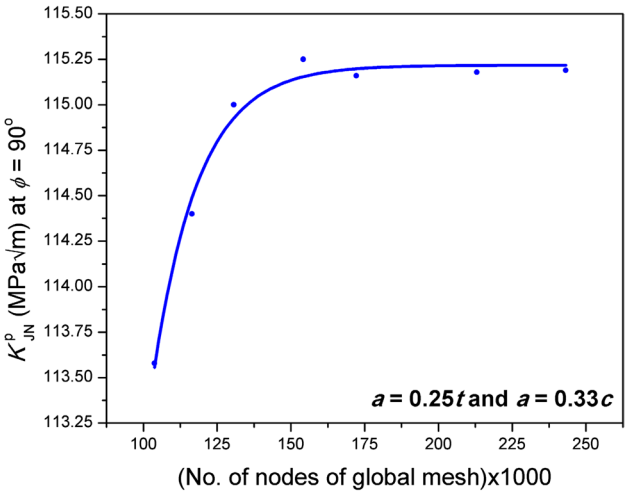

Fig. 11 Mesh-independent study

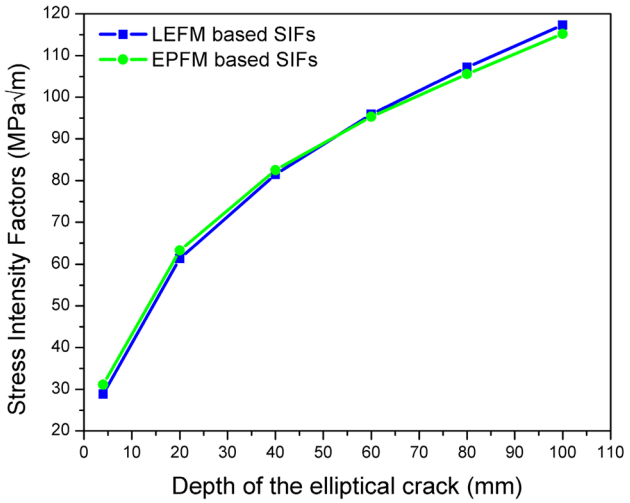

Fig. 12 The comparison between 'LEFM-based SIFs' and 'EPFM-based SIFs'

shows EPFM-based SIFs of the cracks having minor axis (a) equal to 1, 5, 10, 15, 20 and 25 % of the wall thickness (t), respectively. The worst crack ($a = 0.25t$ and $a = 0.33c$) has the EPFM-based maximum SIF equal to $K^{P}_{\mathrm{JN,max}} = 115.23$ Mpa$\sqrt{\mathrm{m}}$ as shown in Fig. 10f.

4.5 Mesh-independent study

The basic mesh-independent study of the 'pallet body fracture model' of the RPV was also conducted. For the demonstration, a corner crack having dimensions '$a = 0.25t$' and '$a = 0.33c$' was taken; and the 'EPFM-based SIF' at the crack tip is presented in Fig. 11. The exponentially growing trend of the SIFs is seen when the number of nodes are increased. The exponentially growing trend predicts that the 'pallet body fracture model' produces good converging and mesh-independent SIFs.

The 'pallet body fracture model' of the RPV having global nodes 175,583 (see Table 3) has been used for the computations of the SIFs. It is evident from Fig. 11 that the fracture model with 175,583 nodes yields converging results.

4.6 The comparison between the two types of SIFs

The comparison of the 'LEFM-based SIFs' with the 'EPFM-based SIFs' has also been performed in order to investigate the effects of material plasticity on the SIFs. For the purpose, both types of SIFs of the cracks having aspect ratio '$a/c = 0.33$' are plotted in the Fig. 12. It is clear from the results that initially up to $a = 52.5$ mm the 'EPFM-based SIFs' are higher than the 'LEFM-based SIFs'. However, for the larger cracks where $a > 52.5$ mm the 'LEFM-based SIFs' are higher than the 'EPFM-based SIFs'. This inverted behavior is due to the fact that for bigger cracks, the plastic zone at the crack tips becomes larger. The larger plastic zones at the crack tip actually blunts the crack tip, which finally leads to the reduction of the SIFs. Hence, the larger plastic zones at crack tips are actually beneficial for the cracks.

4.7 The normalized 'LEFM-based SIFs'

The maximum SIF at the deepest point of a semi-elliptical surface crack in finite plate under remote tension [5] can be evaluated using the following analytical relationship [19].

$$K_{I,\max} = \left(T_F \times \sqrt{\pi a / Q}\right), \tag{1}$$

where 'T_{F}' is the remote tension, 'a' is the crack depth, and 'Q' is the flaw shape parameter [5]. If the remote tension in Eq. (1) is replaced by the hoop stress in a cylindrical portion then the formula can give a close estimation of a maximum SIF of the surface crack in a cylindrical portion [19]. In order to investigate the strength of the corner crack at nozzle–cylinder intersection in comparison to the surface crack in simple cylindrical potions; the SIFs of the corner crack can be normalized according to Eq. (1). If the thickness of the cylindrical portion is taken equal to the nozzle's belt thickness ($t = 400$ mm), then membrane hoop stress in the cylindrical portion can be calculated as $\sigma_{\mathrm{h}} = P_{\mathrm{int}} \times R_{\mathrm{m}} / t = 80.48$ Mpa, where 'P_{int}' is the internal pressure of the RPV (17.16 *MPa*), and 'R_{m}' is the mean radius of the nozzle belt (1876 mm). In this way, SIFs of the corner cracks at the nozzle–cylinder intersection of the RPV can be normalized by dividing them with the term $\left(\sigma_h \times \sqrt{\pi \cdot a / Q}\right)$. The normalization factor, computed in this way, will help to investigate the effects of

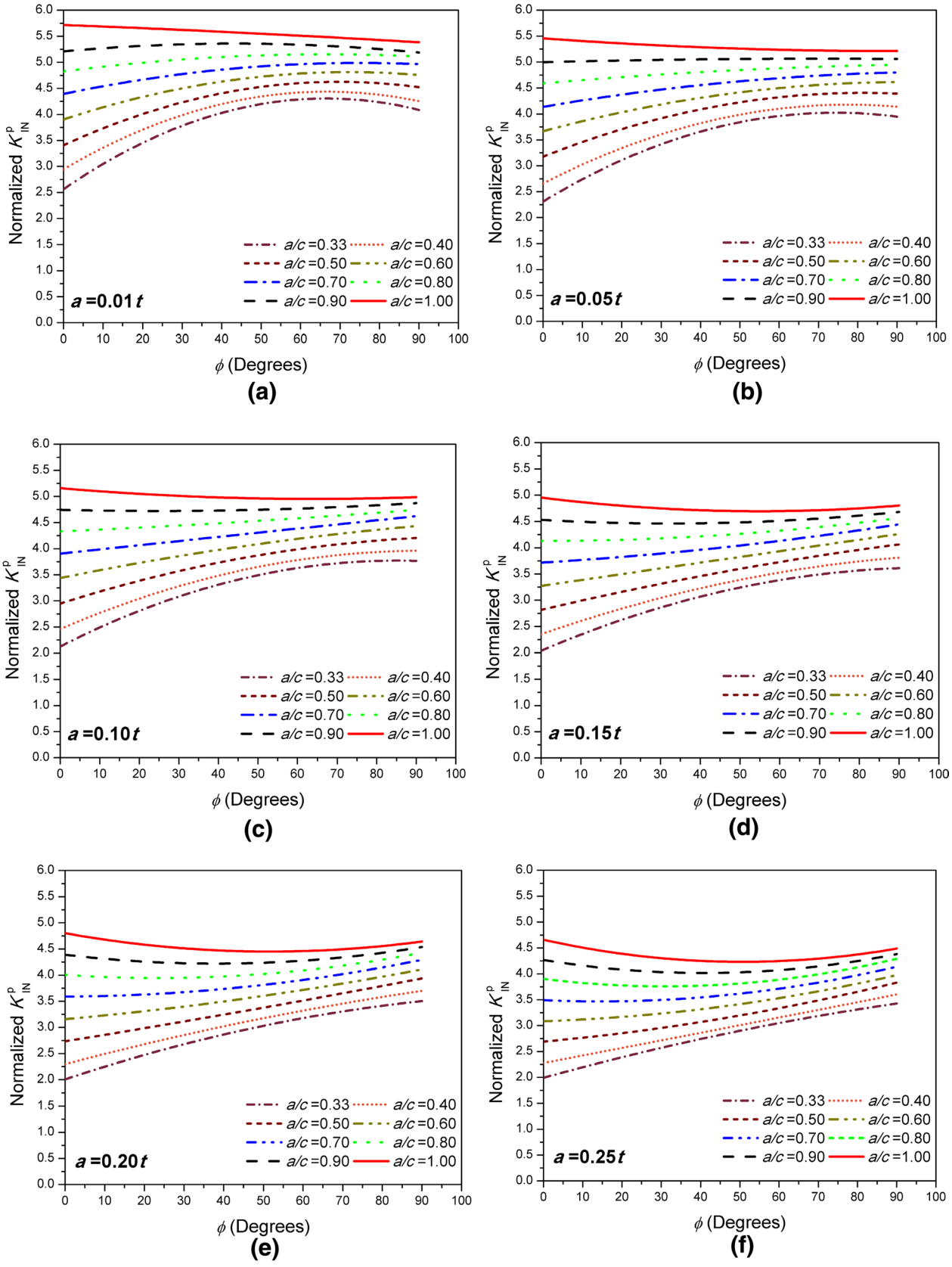

Fig. 13 The normalized LEFM-based SIFs of the corner cracks

stress concentrations around the nozzles, on the SIFs of the cracks.

The normalized 'LEFM-based SIFs' for all the corner cracks listed in Table 2 are presented in Fig. 13. Figure 13a–f shows normalization factors of the corner cracks having minor axis (a) equal to 1, 5, 10, 15, 20 and 25 % of the wall thickness (t), respectively.

It is evident from Fig. 13a–f that the maximum normalization factor is in the case of circular corner crack ($a/c = 1.0$). The circular crack of depth '$a = 0.01t$' has maximum normalization factor which is around 5.7, as shown in Fig. 13a. In comparison to this, circular crack of depth '$a = 0.25t$' has maximum normalization factor which is around 4.7 as shown in Fig. 13f. It means that the larger circular crack has lesser normalization factor. It is due to the fact that larger cracks do have relatively higher cracked area and the effects of stress concentrations are reduced in higher area compared to smaller area. It is also evident from Fig. 13a–f that the minimum normalization factor is in the case of elliptical corner crack having aspect ratio '$a/c = 0.33$'. The elliptical corner crack of depth '$a = 0.25t$' has minimum normalization factor which is around 2.

5 Conclusion

The SIF solutions of the corner surface cracks located at the set-in nozzle–cylinder intersection of a 300-MW reactor pressure vessel (RPV) have been provided in this study. Both the LEFM- and the EPFM-based SIFs are presented in a suitable graphical format. The main conclusions drawn from the study can be summarized as follows:

- The LEFM-based SIFs are not sufficient solutions for the corner cracks in the RPV made of 'SA-508 Gr.3 Cl.1' nuclear-grade steel.
- The material plasticity causes yielding at the crack tip; and therefore forms plastic zones at the crack tips. However, larger plastic zones are beneficial for the cracks; because they actually blunt the crack tips and reduce the SIFs of the cracks.
- The SIFs at the nozzle–cylinder intersection differ significantly from the SIFs of the same cracks located in the cylindrical sections. The normalization factor, in some cases, approaches the value of 5.7.

Acknowledgments The financial support of Pakistan Institute of Engineering and Applied Sciences for the study under IT and Telecom Endowment Fund is gratefully acknowledged.

References

1. Murtaza UT, Hyder MJ (2015) Optimization of the size and shape of the set-in nozzle for a PWR reactor pressure vessel. Nucl Eng Des 284:219–227
2. Murtaza UT, Hyder MJ (2015) Design by analysis versus design by formula of a PWR reactor pressure vessel. International MultiConference of Engineers and Computer Scientists, Hong Kong, pp 942–946
3. ASME Boiler and Pressure Vessel Code (2010) Section III, Division 1: Rules for construction of nuclear facility components
4. Code of Federal Regulations (1996) Fracture toughness requirements for protection against pressurized thermal shock events, Title 10, Part 50, Section 50.61 and Appendix G
5. Murtaza UT, Hyder MJ (2015) The effects of thermal stresses on the elliptical surface cracks in PWR reactor pressure vessel. Theor Appl Fract Mec 75C:124–136
6. Murtaza UT, Hyder MJ (2014) Methodology to analyze 3-D curved surface cracks using hybrid finite elements. International Young Engineers Convention, Lahore, pp 158–165
7. Murtaza UT, Hyder MJ (2016) An approach for the assessment of semi elliptical surface crack. World Congress on Engineering, UK
8. Newman JC Jr, Raju IS (1981) An empirical stress intensity factor equation for the surface crack. Eng Fract Mech 15:185–192
9. ASME Boiler and Pressure Vessel Code (2010) Section XI, Division 1, Non mandatory appendix G: fracture toughness criteria for protection against failure
10. Murtaza UT (2016) Optimization and fracture mechanics analysis of the set-in nozzle of a PWR reactor pressure vessel. Dissertation, Pakistan Institute of Engineering and Applied Sciences
11. Harvey JF (1974) Theory and design of modern pressure vessels. Van Nostrand Reinhold Company, New York
12. He Y, Isozaki T (2000) Fracture mechanics analysis and evaluation for the RPV of the Chinese Qinshan 300 MW NPP under PTS. Nucl Eng Des 201:121–137
13. Haseeb M (2014) Pressure vessel inlet nozzle strength analysis using ANSYS. Dissertation, Pakistan Institute of Engineering and Applied Sciences
14. ASME Boiler and Pressure Vessel Code (2010) Section II, Part D: properties, materials
15. Dieter GE (1987) Mechanical metallurgy. McGraw-Hill, USA
16. Shigley JE (1986) Mechanical engineering design. McGraw-Hill, Singapore
17. Guerrero MA, Betegon C, Belzunce J (2008) Fracture analysis of a pressure vessel made of high strength steel (HSS). Eng Fail Anal 15:208–219
18. Ramesh K (2007) E-Book on engineering fracture mechanics. IIT Madras, India
19. Diamantoudis AT, Labeas GN (2005) Stress intensity factors of semi-elliptical surface cracks in pressure vessels by global-local finite element methodology. Eng Fract Mech 72:1299–1312